Detection of the Free Antineutrino*

F. REINES,† C. L. COWAN, JR.,‡ F. B. HARRISON, A. D. MCGUIRE, AND H. W. KRUSE
Los Alamos Scientific Laboratory, University of California, Los Alamos, New Mexico
(Received July 27, 1959)

The antineutrino absorption reaction $p(\bar{\nu},\beta^+)n$ was observed in two 200-liter water targets each placed between large liquid scintillation detectors and located near a powerful production fission reactor in an antineutrino flux of 1.2×10^{13} cm^{-2} sec^{-1}. The signal, a delayed-coincidence event consisting of the annihilation of the positron followed by the capture of the neutron in cadmium which was dissolved in the water target, was subjected to a variety of tests. These tests demonstrated that reactor-associated events occurred at the rate of 3.0 hr^{-1} for both targets taken together, consistent with expectations; the first pulse of the pair was due to a positron; the second to a neutron; the signal dependended on the presence of protons in the target; and the signal was not due to neutrons or gamma rays from the reactor.

INTRODUCTION

THE importance of a direct verification of the Pauli-Fermi neutrino hypothesis[1] has long been recognized. The experiment reported in this paper was designed to show that the neutrino has an independent existence, i.e., that it can be detected away from the site of its creation, by means of the effect it produces on a counter. In this work, carried out at the Savannah River Plant of the U. S. Atomic Energy Commission, we investigated the reaction[2]

$$\bar{\nu}+p\rightarrow\beta^+ +n, \qquad (1)$$

which is the antineutrino-induced inversion of neutron decay.

The detection scheme is shown schematically in Fig. 1. An antineutrino ($\bar{\nu}$) from the fission products in a powerful production reactor is incident on a water target in which $CdCl_2$ has been dissolved. By reaction (1), the incident $\bar{\nu}$ produces a positron (β^+) and a neutron (n). The positron slows down and annihilates with an electron in a time short compared with the 0.2-μsec resolving time characteristic of our system, and the resulting two 0.5-Mev annihilation gamma rays penetrate the target and are detected in prompt coincidence by the two large scintillation detectors placed on opposite sides of the target. The neutron is moderated by the water and then captured by cadmium in a time dependent on the cadmium concentration (in our experiments practically all neutrons are captured within 10 μsec of their production). The multiple cadmium-capture gammas are detected in prompt coincidence by the two scintillation detectors, yielding a characteristic delayed-coincidence count with the preceding β^+ gammas. The experiment consisted in showing that:

1. Reactor-associated delayed coincidences of the kind described above were observable at a rate consistent with that calculated from the $\bar{\nu}$ flux and the detector efficiency, on the basis of the two-component neutrino theory.
2. The first prompt-coincidence pulse of the delayed-coincidence pair was due to positron-annihilation radiation.
3. The second prompt-coincidence pulse of the delayed-coincidence pair was due to cadmium capture of a neutron.
4. The signal was a function of the number of target protons.
5. The reactor-associated signal was not caused by gamma rays or neutrons from the reactor.

Throughout the experiment an effort was made to provide redundant checks of these several points. Since it may not be easy to repeat the experiment because of the elaborate equipment required, the results are given

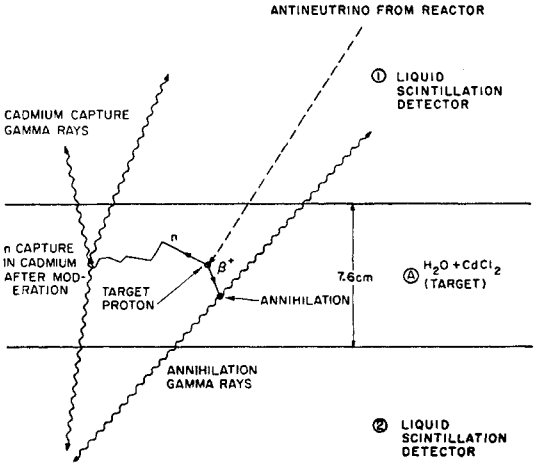

FIG. 1. Schematic diagram of antineutrino experiment.

* Work performed under the auspices of the U. S. Atomic Energy Commission. A preliminary account of the present work appeared in Science **124**, 103 (1956). The antineutrino is generally understood to be associated with negative beta decay.

† Now at the Department of Physics, Case Institute of Technology, Cleveland, Ohio.

‡ Now at the Department of Physics, Catholic University of America, Washington, D. C.

[1] W. Pauli, Jr., address to Group on Radioactivity of Tübingen, December 4, 1930 (unpublished); E. Fermi, Z. Physik **88**, 161 (1934). A discussion of the historical development of the neutrino concept and some pictures of the apparatus used in the present experiment may be found in an article by F. Reines and C. L. Cowan, Jr., Phys. Today **10**, 12 (1957).

[2] A first attempt to study this reaction was made at the Hanford Engineering Works in 1953; F. Reines and C. L. Cowan, Jr., Phys. Rev. **92**, 830 (1953).

below in more than usual detail. In some instances checks which did not give definite positive results were included because it was believed to be important to show that such results were not inconsistent with those expected from antineutrino signals.

EQUIPMENT

A consideration of the cross section for reaction (1) averaged over the fission antineutrino spectrum ($\sim 10^{-43}$ cm^2) and the available $\bar{\nu}$ flux ($\sim 10^{13}$ cm^{-2} sec^{-1}) made it apparent that large numbers of target protons would be required. These were provided by two plastic target tanks containing 200 liters of water each, shaped as slabs 7.6 cm deep and 132 cm by 183 cm in lateral dimensions. Each water tank was sandwiched between two of the three large liquid scintillation detectors (Fig. 2). The thickness of the water tanks was limited by the absorption of the 0.5-Mev positron-annihilation radiation produced in the antineutrino reaction. The array of tanks formed two "triads" with one detector tank in common. The 58-cm depth of the scintillation detectors was chosen so as to absorb the cadmium-capture gammas with the maximum efficiency attainable in the space available for the system. Consideration of light-collection efficiency and the energy resolution required of the system resulted in the use of an extremely transparent liquid scintillation solution containing 3 grams/liter of terphenyl and 0.3 gram/liter of POPOP in highly purified triethylbenzene.[3]

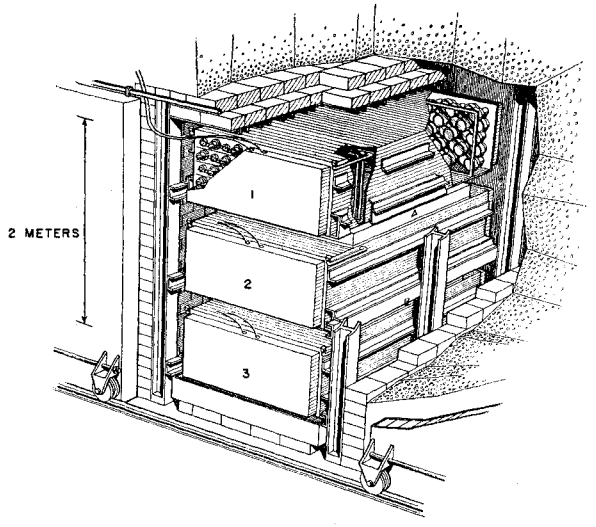

FIG. 2. Sketch of detectors inside their lead shield. The detector tanks marked 1, 2, and 3 contained liquid scintillator solution which was viewed in each tank by 110 5-in. photomultiplier tubes. The white tanks contained the water-cadmium chloride target, and in this picture are some 28 cm deep. These were later replaced by 7.5-cm deep polystyrene tanks, and detectors 1 and 2 were lowered correspondingly. A drip tank, not shown here, was later set underneath tank 3 in the event of a leak. Because of the weight it was necessary to move the lead doors with a hydraulic system.

[3] Ronzio, Cowan, and Reines, Rev. Sci. Instr. 29, 146 (1958).

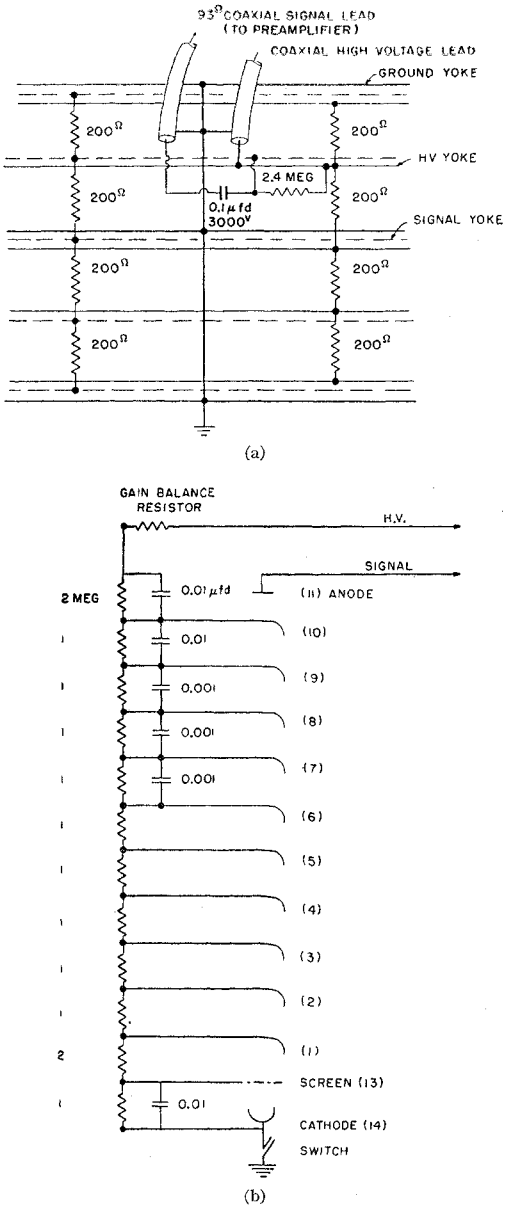

FIG. 3. (a). Schematic of ganging yoke for the 55 photomultiplier tubes at one end of a detector tank. All tubes were connected in parallel across the high-voltage, signal, and ground busses. The 200-ohm parasitic resistors suppressed oscillations. (b) Voltage divider network used on Dumont 6364 photomultiplier tube. These tubes were selected for low noise and their gains were matched by using a standard source and choosing an appropriate value for the gain balance resistor.

The tank walls were painted white, and each tank had 110 5-in. Dumont 6364 photomultipliers (55 on each end) for collection of the scintillation light. The tubes were placed an average distance of about 28 cm behind a plastic window and were immersed in light-matching triethylbenzene which could be made to scintillate, if desired, by the addition of terphenyl and POPOP. Model tests indicated that the non-

uniformity of light collection throughout the tank introduced a pulse-height spread of approximately $\pm 7\%$. Figure 2 shows a sketch of the detectors set into their lead shield. The lead side walls and floor were 10.2 cm thick, the roof 20.3 cm thick, and the doors 20.3 cm (toward the reactor) and 15.2 cm (away from the reactor). The 5400-liter capacity of the detectors required scintillation-liquid storage tanks and pumping facilities at the reactor site. Stainless steel pipes transferred the liquids some 75 meters from the outside storage tanks to the detector inside the reactor building. The detector was filled after emplacement in the shield.

Figures 3(a) shows the electrical ganging yoke for the 55 photomultiplier tubes on one end of a detector tank. The tubes were checked individually prior to insertion in the tank. Noisy ones were rejected, and the gains were balanced by means of a resistor in the high-voltage circuit at each tube shown in Fig. 3(b). The 110 tubes of each tank were operated in parallel.

Scintillation light in the detector was translated into electrical impulses by the photomultipliers on each tank, passed to preamplifiers, and then sent via coaxial cables to the remainder of the electronics located in a trailer van outside the building. Isolation from electrical noise in the local power system was achieved by the use of a separate motor-generator set for all electronic power. Figure 4 is a schematic diagram of the electronic system.

To illustrate how the system functioned, we trace through a typical antineutrino-induced event: Let an event occur in the top target (A), producing a positron and a neutron by reaction (1). The sequence is analyzed by the equipment as follows: First, two pulses from the positron annihilation arise on the signal lines of counters 1 and 2, are amplified by the top triad amplifiers 1β and 2β, and are accepted by the "top β^+ coincidence unit" if in the proper energy gates (0.2 to 0.6 Mev) and in time coincidence (<0.2 μsec apart). This unit informs the "top n coincidence unit" that it has received a β^+-like pulse by sending a pulse which opens a gate in the n unit approximately 30 μsec long. The second pair of prompt-coincidence pulses from 1 and 2 due to neutron-capture gamma rays is accepted by the neutron-coincidence unit if they have the correct energies (>0.2 Mev in each tank with a total from 3 to 11 Mev; the neutron bounds were also operated in some runs with 1.5 to 7 Mev required in each tank). If the second pulse occurs between 0.75 and 30 μsec after the first, the neutron unit announces the completion of the delayed-coincidence event by activating a scaler and triggering the sweeps of the recording oscilloscopes.

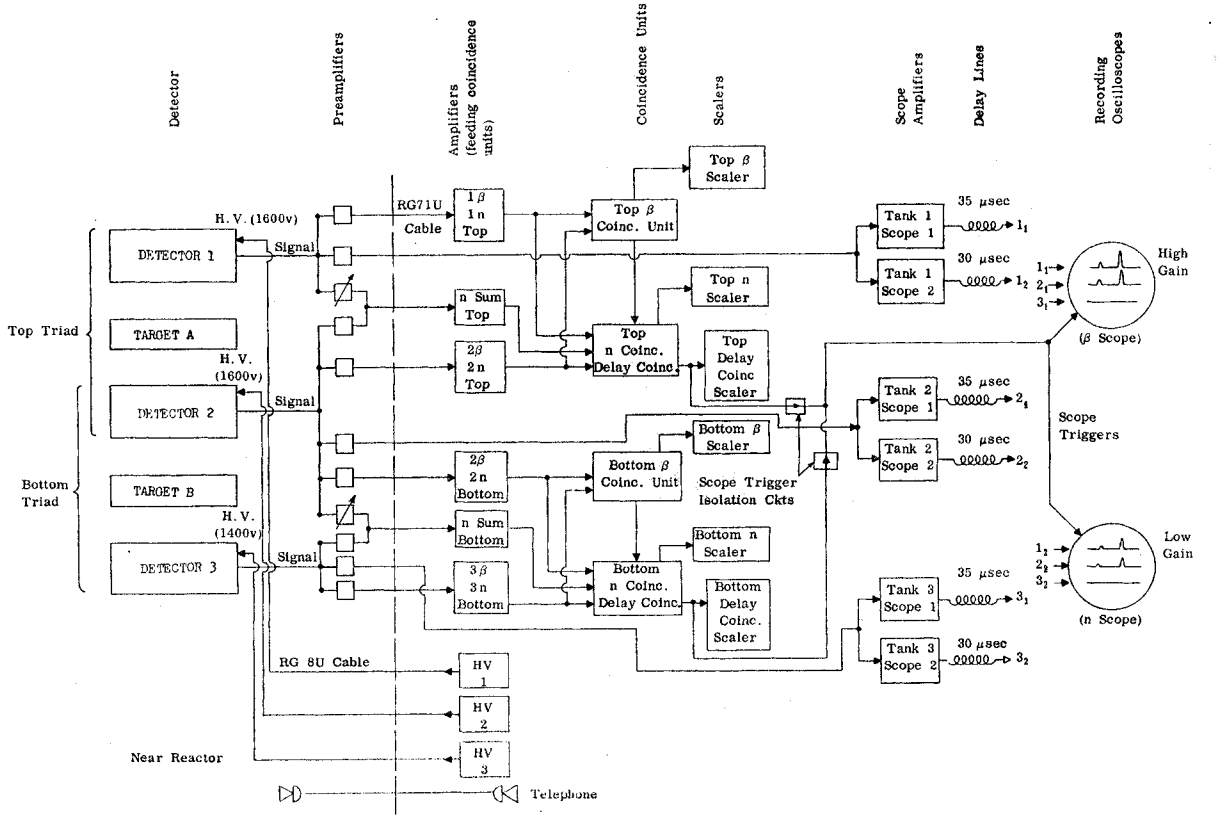

FIG. 4. Schematic diagram of detector and associated electronics.

During this process of selection the signals from the tanks have been stored on delay lines for presentation on the oscilloscope when the signal meets the acceptance requirements. To facilitate determination of the accidental delayed coincidence rate, the β^+- and n-like prompt coincidences are recorded on separate scalers. Film records of each oscilloscope trace were made on 35-mm linagraph ortho film. The camera-frame advance was controlled by the scope trigger. Typical anti-neutrino-induced events are shown in Figs. 5(a) and 5(b). Figures 5(c) shows calibration frames, and Figs. 5(d) through 5(g) are examples of rejected frames.

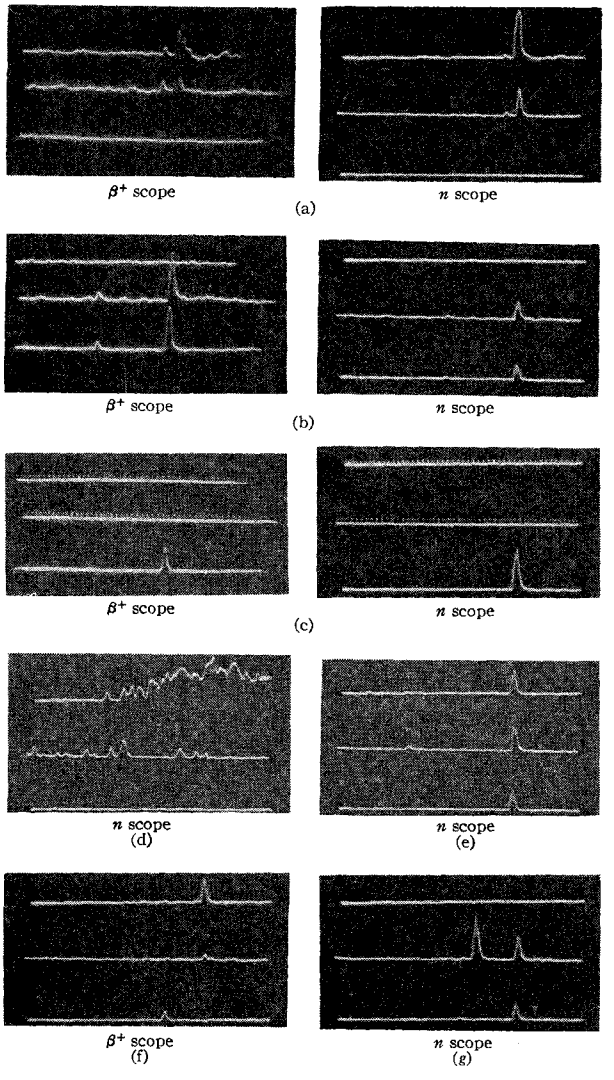

FIG. 5. Sample scope pictures. (a) and (b) are acceptable frames (possible $\bar{\nu}$ events); (c) shows a set of calibration traces; and (d) through (g) are not acceptable. (a) Event in top triad. Delay, 2.5 μsec. First pulse, 0.30 Mev in 1, 0.35 Mev in 2. Second pulse, 5.8 Mev in 1, 3.3 Mev in 2. (b) Event in bottom triad. Delay, 13.5 μsec. First pulse, 0.25 Mev in 2, 0.30 Mev in 3. Second pulse, 2.0 Mev in 2, 1.7 Mev in 3. (c) 0.5-μsec timing markers on traces 1 and 2, 5-Mev (n scope) and 1-Mev (β scope) calibration markers on trace 3. (d) Electrical noise. (e) Cosmic-ray event, "neutron triple." (f) Cosmic-ray event "positron triple." (g) Event, possible due to cosmic rays. Rejected because of an extra pulse but otherwise acceptable. Frames like this occurred more often than would be expected from chance coincidences, but not often enough so that their omission would affect the results appreciably.

CALIBRATION, SYSTEM CHECKS, AND OPERATING PROCEDURE

The energy calibration of the system was obtained by means of the peaks in the energy spectrum resulting from the passage through the tanks of relativistic cosmic-ray μ-mesons, "meson-through peaks." Figures 6(a) and 6(b) show the singles spectra and the spectrum

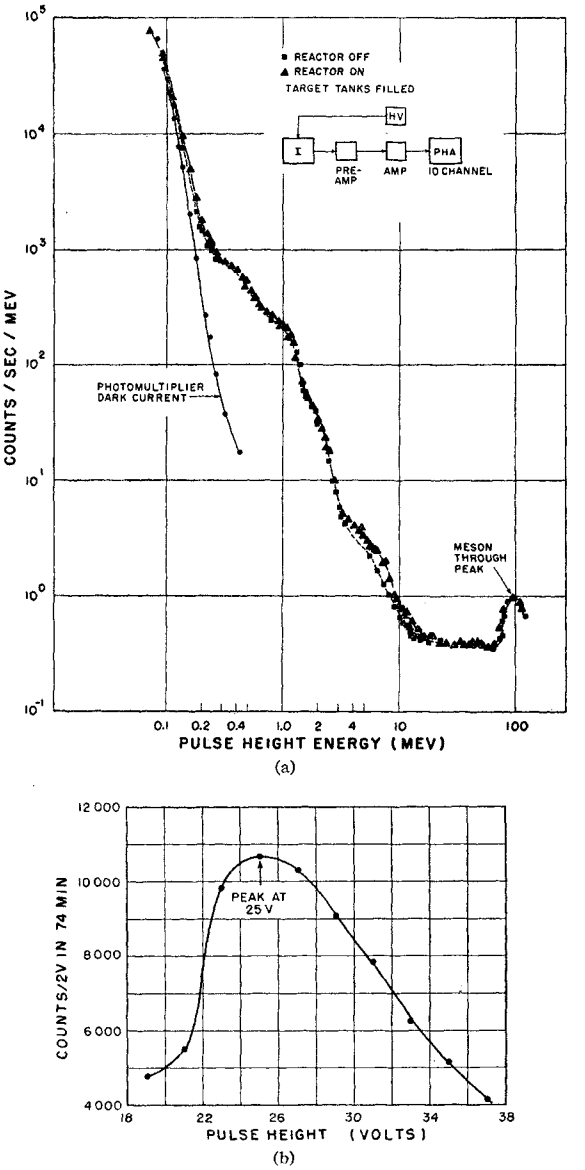

FIG. 6. (a) Detector tank 2 spectrum of single pulses. (b) "Meson through peak": spectrum of pulses in detector tank 2 due to cosmic rays. The pulse-height analyzer was gated by coincidences between tanks 1 and 2.

TABLE I. Summary of first series.[a]

Triad	$\bar{\nu}$ flux[b] factor	Run length (hr)	Total counts	Calculated accidental counts	Net rate (hr^{-1})
(a) Top	1.03	192.7	283	114	0.88±0.10
Bottom	1.04	171.8	224	95	0.75±0.10
(b) Top	0	67.3	55	31.8	0.34±0.14
Bottom	0	69.7	44	39.7	0.06±0.13
(c) Top	0	63.2	48	27.6	0.32±0.14
Bottom	0	63.2	38	35.3	0.04±0.14
(d) Top	1.07	264.5	320	124.9	0.74±0.08
Bottom	1.07	264.5	302	157.2	0.55±0.08

[a] Listings (a) and (b) are directly comparable. During (c) and (d) small changes were made in the operating conditions to reduce the background. See Appendix I.

[b] The $\bar{\nu}$ flux factor is a number proportional to the $\bar{\nu}$ flux.

in the vicinity of the through peak. By matching the pulse heights at which the through peaks were located with a precision pulser, energy bounds were set on discriminator circuits and film calibrations were made. The energy scales were set by multiplying the scintillator depth (~58 cm) by the rate of meson energy loss (1.6 Mev/cm) and allowing for a small (5%) increase in the peak position due to the fluctuation in energy loss and the angular distribution of the incident muons.

Through peaks were run at regular intervals and the system was checked and aligned at weekly intervals on the average. During the five-month period of the experiment a downward drift of a factor of 2 was noted in the gain of the detectors. The energy calibrations given by the through peaks are estimated to be accurate to within 10%, and these peaks were used to check the stability of the system during a particular run. The efficiency of the system for detecting positrons and neutrons was determined using positron and neutron sources.

DEMONSTRATION OF REACTOR-ASSOCIATED SIGNAL

The measurenents made to demonstrate the existence of a $\bar{\nu}$-like signal and its dependence on reactor power, and hence on $\bar{\nu}$ flux, were made in two series. In the first series some of the parameters were being changed to optimize the operating conditions. The results of this series are shown in Table I. The changes were not expected to alter the net counting rate greatly, and, indeed, the rate stays approximately constant throughout the series. Since we do not in this series attempt to establish absolute rates, the analysis of the data is greatly simplified. For example, in computing accidental-background rates we overcorrect the data if we do not allow for that fraction of spurious accidental counts (e.g., the very occasional traces counting noise-hash) which have already been excluded by the process of film selection. Since the number of accidentals is slightly greater when the reactor is on we err on the side of reducing the reactor-associated correlated signal rate by overcorrecting the data for accidentals in this way.

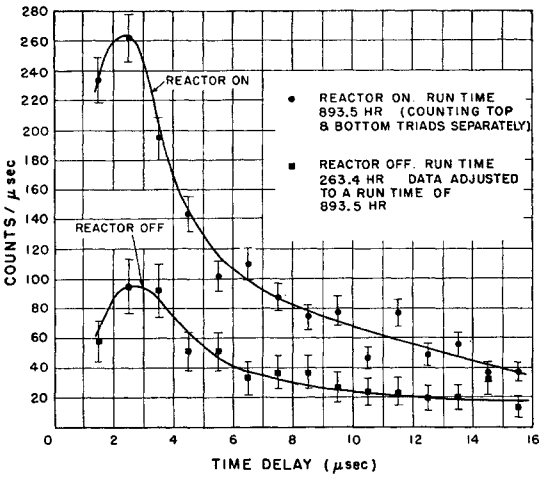

FIG. 7. Time-delay spectrum first series. Curves show theoretical distribution for $\alpha=0.005$ plus accidental background. Theoretical calculations are not considered reliable beyond 10 μsec because statistical errors in Monte Carlo method increase with decreasing sample available in that range.

For the first part of the series [(a) and (b)] the total net rate (reactor on minus reactor off) was 1.23±0.24 hr^{-1}. For the second part [(c) and (d)] (during which small changes were being made) the net rate was 0.93±0.22. From these data we conclude that there was a reactor-associated signal.

Figure 7 shows the distribution of time-delay intervals from these runs. Throughout this series, the cadmium concentration was $\alpha=0.005$, where α is the cadmium-hydrogen atomic ratio in the solution.

At the start of the second series a number of changes were made to increase the antineutrino signal and lower the background:

1. The cadmium concentration was increased to make $\alpha=0.010$.
2. The neutron-detection efficiency was increased by setting the lower bounds of the neutron gates to 0.2 Mev with no upper limit requirements and by adding a "sum" coincidence system which requires the total neutron energy in each triad to lie between 3 and 11 Mev.
3. Additional lead was placed above the detector tanks, and the target tanks were surrounded by approximately 730 kg of paraffin.
4. The delayed-coincidence gate was lengthened from 15 to 30 μsec to allow a better assessment of accidental background.
5. The long upper gate was shortened to 60 μsec and was fixed to stay on for this time following not only a too-large pulse but also the end of an overdriven "bustle." See Appendix I.

The data from series 2 and part of series 3 are given in the histograms of Fig. 8, which show the time-delay distribution for each triad with reactor on and reactor off. Table II summarizes the data for this series.

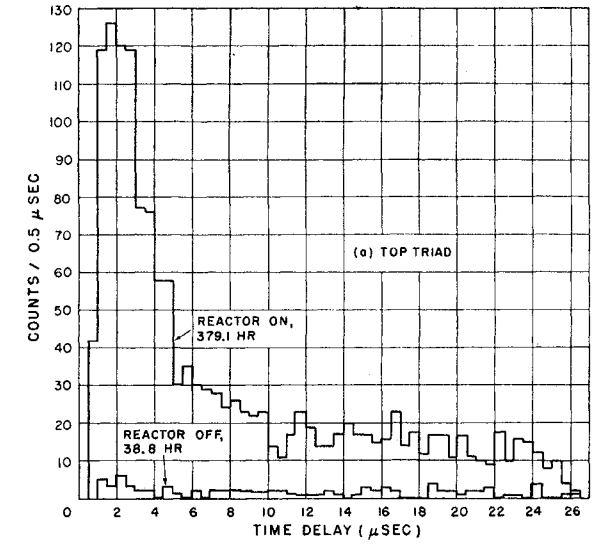

FIG. 8. (a) Top triad, series 2 and 3b. Time-delay distribution: $\alpha=0.010$, H_2O+Cd. For reactor on: $\bar{\nu}$ flux factor, 1.13; counts from 0.75 to 7 μsec, 919; from 11 to 25 μsec, 427. For reactor off: counts from 0.75 to 7 μsec, 27; from 11 to 25 μsec, 40. (b) Bottom triad, series 2 and 3b. Time-delay distribution: $\alpha=0.010$, H_2O +Cd. For reactor on: $\bar{\nu}$ flux factor, 1.12; counts from 0.75 to 7 μsec, 815; from 11 to 25 μsec, 398. For reactor off: counts from 0.75 to 7 μsec, 119; from 11 to 15 μsec, 145.

For $\alpha=0.01$, over 95% of the neutrons have been captured by 11 μsec.[4] The counts in the time-delay interval from 11 to 25 μsec were taken to be accidental. In this series, only the counts in the interval from 0.75 to 7 μsec were counted as signals, and the accidental rate was derived from the counts in the interval from 11 to 25 μsec, multiplied by the correction factor 6.25/14.

Subtraction of the reactor-independent time-correlated background (flux factor=0) from the net counting rates (flux factor=1.13, 1.12) gives 1.69 ± 0.17 hr^{-1} for the top-triad signal rate and 1.24 ± 0.12 hr^{-1} for the bottom triad. The ratio of signal to accidental background is about 4:1, and the ratio of signal to reactor-independent correlated background is about 5:1. The reactor-associated increase of the accidental background is less than 0.05 hr^{-1}, i.e., less than 1/25 of the signal.

Because of the difference in the distances from the reactor to the two target tanks, the $\bar{\nu}$ counting rate is expected to be about 10% higher in the upper triad. After correction for this factor, the ratio of the rates is 1.24 ± 0.17, a value not inconsistent with unity.

EXPECTED COUNTING RATE

Although it was not the purpose of this experiment to make a precise determination of the $\bar{\nu}$-interaction cross section,[5] it nevertheless is important to establish that the counting rates observed were consistent with the expected cross section. For this purpose it is necessary to know the efficiency with which neutrons and positrons were detected.

Neutron Detection Efficiency

An attempt was made to determine the neutron-detection efficiency by studying the response of the apparatus to a Pu-Be neutron source. Unfortunately, the neutrons from this source differed in two essential ways from the neutrons produced in our reaction:

(1) The Pu-Be neutrons are of higher energy, ranging up to about 11 Mev;[6] neutrons from our reaction[7] are of the order of 10 kev.

(2) The Pu-Be source is a point source, whereas the $\bar{\nu}$-associated neutrons are produced uniformly throughout the target volume.

The second of these differences was eliminated in part by placing the source in several positions on top of the target tank and averaging the response. No simple, precise approach is available to take account of the differing spectra.

First the relative neutron-detection efficiencies were measured for various source positions on the water

TABLE II. Summary of second series.

Triad	$\bar{\nu}$ flux factor	Run length (hr)	Counts from 0.75–7 μsec	Counts from 11–25 μsec	Accidental background (hr^{-1})	Net rate (hr^{-1})
Top	1.13	379.1	919	427	0.50±0.02	1.92±0.09
	0	38.8	27	40	0.46±0.07	0.23±0.15
Bottom	1.12	383.5	815	398	0.46±0.02	1.66±0.08
	0	128.0	119	145	0.50±0.04	0.42±0.09

[4] Reines, Cowan, Harrison, and Carter, Rev. Sci. Instr. **25**, 1061 (1954).

[5] A more accurate cross-section measurement made subsequently to that reported here is the subject of a paper by F. Reines and C. L. Cowan, Jr., Phys. Rev. **113**, 273 (1959).

[6] Leona Stewart, Phys. Rev. **98**, 740 (1955).

[7] The neutron spectrum associated with fission-fragment antineutrinos is discussed in Appendix II.

target, as indicated in Fig. 9. Then a measurement was made of the detection efficiency for a centrally placed source. The neutron source was placed on top of target tank B, and the rates measured on the bottom n scaler (Fig. 4).

Counting rates were measured for pulses satisfying the coincidence condition that $2n$ and $3n$ separately be >0.1 Mev, and the sum $(2n+3n)$ between 3 and 11 Mev. The measurements consisted of scaler readings obtained with and without cadmium in the water target. Table III shows the results.

Since the source strength was 3100 sec^{-1}, the accidental background rates were negligible. With no cadmium, a part of the counting rate was due to neutrons which would have been captured in the cadmium, a part to those which would not, and a part to gamma rays from the source. Only part of the counting rate without cadmium should therefore be subtracted as background. The similarity of the figures in the last two columns of Table III makes us believe that this source of error is unimportant.

The average efficiency of the detector relative to a central source was calculated from these data in two ways: first, the positions were weighted according to the symmetry they represent, e.g., position 5 was given weight 4; and second, all positions were given equal weight (thus weighting areas near the center more heavily). For unequally weighted points the average efficiency was 0.60; equal weighting gave 0.64. The closeness of these results gives confidence in the value 0.60.

Neutron-Detection Efficiency for the Central Position

In the $Be^9(\alpha,n)C^{12}$ reaction, the C^{12} is left in an excited state and about one-third of the time returns to the ground state with the emission of a 4.5-Mev gamma ray. The detection efficiency for neutrons produced by the Pu-Be source in the central position (on top of tank B) was measured by determining in what fraction of cases a 4.5-Mev gamma pulse in tank 2 was followed by a neutron pulse in tanks 2 and 3. The bottom β coincidence unit (see Fig. 4) was used as a discriminator

TABLE III. Relative response *vs* neutron-source position.

Source position	Counts/sec with Cd	Counts/sec without Cd	Net[a]	Response relative to position 1: Net/net for position 1	Response relative to position 1: Gross/gross for position 1
1	530	192	338	1.00	1.00
2	260	90	170	0.50	0.49
3	130	55	75	0.22	0.25
4	250	90	160	0.47	0.47
5	450	175	275	0.81	0.85
6	260	105	155	0.46	0.49
7	230	90	140	0.41	0.43
8	470	163	307	0.91	0.89
9	516	195	321	0.95	0.97

[a] Background with source removed is 6 counts/sec.

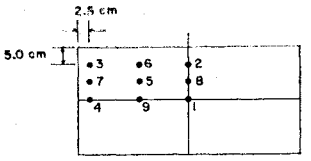

FIG. 9. Various source positions on top of the water target.

for the gamma-ray pulses. Neutrons were detected in the usual way with the "bottom n coincidence, delay coincidence" unit. The first-pulse rate was, in fact, due not only to the 4.5-Mev gammas from the excited carbon level but also to neutron-capture gamma rays and background gamma rays not associated with the source. The first-pulse rate with the source and without cadmium in the target water was 329 sec^{-1}; with cadmium in the target water the rate was 390 sec^{-1}. Without cadmium or the neutron source the first-pulse rate was 10 sec^{-1}. Since cadmium made such a small change, the counts due to neutron capture in the ion of the tanks in the vicinity of the source were neglected, and the number used for the first-pulse rate due to the 4.5-Mev gamma directly from the neutron source was 319 sec^{-1}.

With a gate length of 11.5 μsec, the counting rate was measured to be 43.0 sec^{-1} for pulses satisfying the coincidence condition that $2n$ and $3n$ separately be >0.1 Mev, and the sum $(2n+3n)$ between 0.92 and 11 Mev. Correcting this number for the fraction, 0.56, of these capture pulses with a sum >3 Mev (as determined by pulse-height analysis of the capture-gamma spectrum) and allowing for the fact that only 0.93 as many neutrons are captured[4] in 0.75 to 7 μsec, we find the efficiency for the centrally placed Pu-Be source to be

$$100\times0.56\times43.0\times0.93/319=7.0\%.$$

Since only one-half of the neutrons were headed towards the target tank, the true detection efficiency for the Pu-Be source was 14%. This is a lower limit for the detection efficiency of $\bar{\nu}$-produced neutrons both because of the difference in the neutron-energy spectrum, and because we used an upper limit for the gamma-ray counting rate.

The detection efficiency appropriate to $\bar{\nu}$-produced neutrons will now be estimated in an *a priori* manner and the result compared with the lower limit of 14% given above. The efficiency ϵ_n' can be written as a product of three terms:

$$\epsilon_n' = \epsilon_1\epsilon_2\epsilon_3, \tag{2}$$

where ϵ_1 is the probability a neutron will not leak out of the water target, ϵ_2 is the probability that the neutron will be captured by the cadmium in the time during which the system is sensitive, and ϵ_3 is the probability that the gamma rays resulting from neutron capture will satisfy the coincidence requirements.

The mean free path for 10-kev neutrons in the target is 0.75 cm. Assume that all neutrons produced within

0.75 cm of the target edge are captured with 70% efficiency, and those produced in the central 6.1 cm are captured with 100% efficiency. This gives the value for $\epsilon_1=0.94$.

From Monte Carlo calculations[4] and a measurement of the time-delay distribution with a neutron source, the neutron-capture efficiency in the gate time of 0.75 to 7 μsec is $\epsilon_2=0.86$.

To estimate ϵ_3 which is the least certain of all, consider the gamma rays from neutron capture in cadmium. The average multiplicity[8] is 4. If we require >0.2 Mev on each side, with the sum between 3 and 11 Mev, then at least one gamma ray must be detected by each detector. The probability of this (assuming no angular correlation of the gammas or self-absorption by the target) is 0.87, which is an overestimate. Even if the gamma rays were directed so as to make possible a coincidence, this does not ensure neutron detection because of the chance that the total energy loss suffered by the gammas in the detectors may be <3 Mev. It appears from the experiment with the Pu-Be source that only 0.56 of these gamma rays, with a total energy >0.92 Mev, satisfy the energy criteria (neglecting the change in side gates from 0.1 to 0.2 Mev). Hence

$$\epsilon_3=0.87\times0.56=0.49,$$

and finally

$$\epsilon_n'=0.94\times0.86\times0.49=0.40,$$

to be compared with the experimental lower limit of 0.14. Combining this number with the 0.60 relative figure for the efficiency averaged over the target tank area, we obtain as a rough estimate for the over-all detection efficiency of the system for $\bar{\nu}$-produced neutrons

$$\epsilon_n=0.40\times0.60=0.24.$$

It seems reasonable to state the efficiency as

$$\epsilon_n=0.17\pm0.06,$$

where 0.06 represents a guess as to the uncertainty of ϵ_n.

Positron-Detection Efficiency

The positron-detection efficiency was determined by dissolving a known amount of β^+ emitter, Cu^{64}, in the water targets and measuring the counting rate of prompt coincidences in the pair of detectors next to each target. Because of the negligibly short range of the Cu^{64} positrons as compared with the more energetic β^+ from the $\bar{\nu}$ reaction, the detection efficiency for $\bar{\nu}$-produced positrons was 0.9 times that for Cu^{64} positrons (see Appendix III).

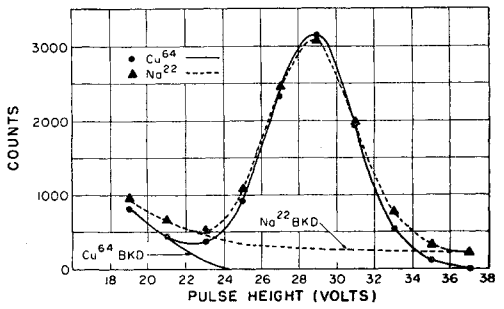

FIG. 10. Comparison of Cu^{64} and Na^{22} β^+ sources.

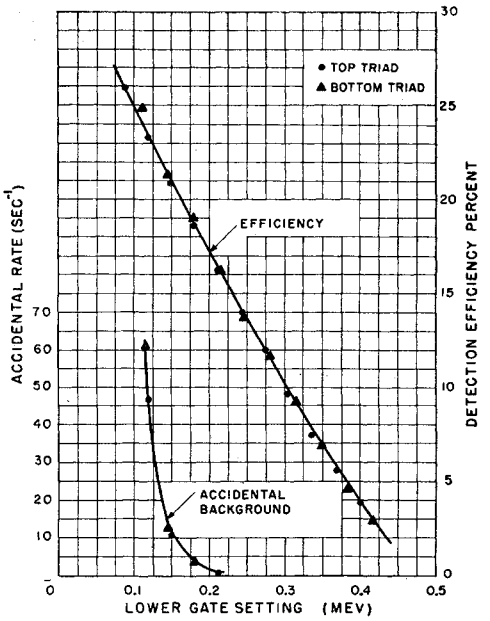

FIG. 11. Positron-detection efficiency and accidental background *vs* lower-gate setting in β coincidence unit.

The calibration consisted of two parts: the measurement of the response to the Cu^{64} source and the determination of the source strength by comparison with a Na^{22} standard.[9] The β^+ emitter with which we compared the Cu^{64} sources[10] was a standard stock solution of Na^{22} as $Na^{22}Cl$ provided by B. J. Dropesky of Los Alamos. Our standard had a specific activity of 1550 $\pm$75 disintegrations per second per gram of solution when used. Comparisons were made of the Cu^{64} and Na^{22} source strengths by placing the samples in a standard geometry near a $1\frac{1}{2}$-in.-diameter, $\frac{1}{2}$-in. thick NaI crystal viewed by a 2-in. (Dumont 6292) photomultiplier.

The intercomparison consisted in making a pulse-height analysis of the annihilation radiation from 1.023 *g* of Na^{22} source solution (1580$\pm$80 β^+/sec) and 1.44 g of solution containing Cu^{64} as $Cu^{64}NO_3$. Figure 10 shows the two spectra obtained after nonsource-associated backgrounds were subtracted. The estimated

[8] C. O. Muehlhause, Phys. Rev. **79**, 277 (1950).

[9] The characteristics of these sources and references to the original literature may be found in the compendium by Strominger, Hollander, and Seaborg, Revs. Modern Phys. **30**, 585 (1958).

[10] These Cu^{64} sources were prepared by irradiation in the neutron flux of the Savannah River Laboratory test reactor. We wish to thank Dr. G. Dessauer and his staff for their cooperation in the use of this facility.

source-associated backgrounds are also shown on the figure; the small tail on the high-energy side of the Na^{22} curve is probably due to the Na^{22} gamma activity. After background subtraction, the ratio of counts was found to be 1.07, giving an initial specific activity for the Cu^{64} solution of 1170 β^+/g-sec. Then 6.47 g of solution was put in tank A (7600 β^+/sec) and 6.90 g of solution in tank B (8100 β^+/sec). By the time the triads were measured, the sources had decayed to 1930 β^+/sec (A) and 1960 β^+/sec (B). The response of the system to β^+-annihilation radiation seen in coincidence was measured as a function of the lower-gate setting on the coincidence units. Figure 11 shows the detection efficiencies of the two triads given by the scaler readings and a knowledge of the β^+-decay rates. The upper gates were kept fixed at 0.6 Mev and the lower gates were moved keeping the two energies equal. The accidental backgrounds were determined by inserting a 0.27-μsec delay in the signals from one detector of a pair. Energy gates chosen for the $\bar{\nu}$ runs with a view to reducing accidental backgrounds were 0.2 to 0.6 Mev and corresponded to a β^+-detection efficiency of 17% for Cu^{64} positrons with an uncertainty less than $\pm 10\%$. If allowance is made for leakage of β^+ associated with $\bar{\nu}$-induced events, this figure is reduced to $15\pm 2\%$.

Cross Section

Using our experimental numbers, we are now in a position to calculate the cross section for the reaction $p(\bar{\nu},\beta^+)n$ induced by antineutrinos from fission fragments. As pointed out above, our object is only to check whether the cross section which we deduce from our experiment is consistent with expectations. The cross section, σ, is calculated from the equation

$$\sigma = \frac{R}{3600 F N \epsilon_n \epsilon_\beta} \text{ cm}^2, \qquad (3)$$

where $R = 1.5\pm 0.1$ hr^{-1}, the average signal rate per triad, $\epsilon_n = 0.17\pm 0.06$, $\epsilon_\beta = 0.15\pm 0.02$, $N = 1.1\times 10^{28}$, the number of hydrogen nuclei in each target tank, and $F = 1.2\times 10^{13}$ cm^{-2} sec^{-1}, the average $\bar{\nu}$ flux at the detector.[11] Therefore

$$\sigma = \frac{1.5\pm 0.1}{3600\times 1.2\times 10^{13}\times 1.1\times 10^{28}(0.17\pm 0.06)(0.15\pm 0.02)},$$

$$\sigma = (1.2_{-0.4}{}^{+0.7})\times 10^{-43} \text{ cm}^2.$$

This value is in agreement with the theoretically expected value[12] of $(1.0\pm 0.17)\times 10^{-43}$ cm^2.

TABLE IV. Lead absorption experiment.

$\bar{\nu}$ flux factor	Pb thickness (cm)	Run length (hr)	Counts from 0.75–7 μsec	Counts from 7–25 μsec	Signal + bkd. rate (hr^{-1})	Accidental bkd. (hr^{-1})
1.00	0	383.5	815	542	2.13±0.07	0.49±0.02
1.00	0.16	118.4	153	118	1.29±0.10	0.35±0.03
1.02	0.48	54.1	52	45	0.96±0.13	0.29±0.04
1.04	0.95	311.5	151	207	0.48±0.04	0.23±0.02
0	0	128.0	119	185	0.93±0.09	0.50±0.04
	0.95	59.9	19	50	0.32±0.07	0.29±0.04

TABLE V. Signal rates for lead absorption experiment.

Pb thickness (cm)	Signal (hr^{-1})
0	1.24±0.12
0.16	0.62±0.14
0.48	0.40±0.16
0.95	0.04±0.07

EVIDENCE THAT THE FIRST PULSE WAS DUE TO A POSITRON

An experiment was done to determine whether the first pulse of the delayed-coincidence pair was due to β^+-annihilation radiation. It consisted of putting various thicknesses of lead sheet between target tank B and detector 2 and observing the diminution of the reactor-associated signal. The results are shown in Table IV. The accidental background rates in the 0.75- to 7-μsec channel (column 7) were calculated by multiplying the rates in the 7- to 25-μsec channel by 6.25/18.

In order to calculate the reactor-associated signal rates for each thickness of lead, we need values for the total backgrounds. For the case with the best statistics (no lead) the accidental background is, within a few percent, independent of reactor power. On this basis we estimate the total background, including correlated events, by multiplying the accidental rates for each thickness of lead by the ratio observed with no lead: (total background rate)/(accidental rate) = 0.93/0.49 = 1.90. The errors are statistical and take no account of the uncertainty in the method of estimating the background. This, together with an allowance for the small differences in $\bar{\nu}$ flux, gives the results of Table V. The statistically poorer datum (19 counts) from the run with 0.95 cm of lead with the reactor off was disregarded in the analysis.

The reduction in over-all detection efficiency with increasing thickness of lead is due primarily to the attenuation of the β^+-annihilation radiation and to a lesser extent to the attenuation of the gamma rays associated with neutron capture in cadmium. In order to determine the first factor, a mockup experiment was performed. This experiment consisted in measuring the response of a NaI crystal placed above the middle

[11] The $\bar{\nu}$ flux at the detector is calculated from a knowledge of the reactor power, the energy per fission, the number of $\bar{\nu}$ per fission (6.1), and the distance from the center of the reactor to the proton target.

[12] Carter, Reines, Wagner, and Wyman, Phys. Rev. **113**, 208 (1959).

TABLE VI. Absorption experiments with sources.

Pb thickness (cm)	Relative β^+ signal	Relative n signal	Relative $\bar{\nu}$ signal Predicted	Observed
0	1.00	1.00	1.00	1.00
0.16	0.47	(0.86)	0.40	0.50±0.13
0.48	0.17	0.68	0.12	0.32±0.14
0.95	0.04	0.45	0.02	0.03±0.06

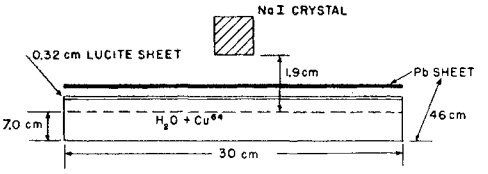

FIG. 12. Experimental mockup of detector for measurement of absorption by lead of β^+-annihilation radiation from Cu^{64}.

of a water tank (containing a dissolved Cu^{64} source) as a function of the thickness of lead sheet interposed between tank and detector. The arrangement is shown in Fig. 12. Results of this measurement are shown in Table VI, column 2.

The difference in the energy resolution of a NaI crystal and a large detector tank makes for an uncertainty in the interpretation of these results in terms of the large detector. However, the insensitivity of the mockup ratios to the lower energy bound settings indicates this uncertainty to be less than ±20%. The tabulated ratios are in accord with what might be expected for the transmission of 0.5-Mev gamma rays isotropically incident on lead sheet of the listed thickness.

The response of the lower triad to a neutron source placed at the top center of the water-$CdCl_2$ target is shown in Table VI, column 3, as a function of lead thickness. The figure for 0.16 cm of lead was not measured, so a calculated number has been inserted in parentheses. The calculations were made assuming at least one gamma ray in each detector, with a multiplicity of three gammas per neutron capture. The calculated and measured values were in agreement for the other thicknesses of lead.

The factor by which the $\bar{\nu}$-detection efficiency may be expected to be reduced is the product of the numbers in columns 2 and 3, and is given in column 4. Column 5 gives the observed ratio, taken directly from Table V. The last two columns agree as well as might be expected in view of the uncertainties enumerated above.

These results support the conclusion that the first pulse of the delayed coincidence pair is due to β^+-annihilation radiation, and may be used to rule out other conceivable sources for the reactor-associated signal, such as neutrons.

Pulse-Height Spectrum

The pulse-height spectrum of the first pulses of $\bar{\nu}$-like events was examined to see if it was consistent with the spectrum to be expected from annihilation radiation. The pulses from each detector were listed separately, the pulse height being measured on the film. The results of the analysis are shown in Table VII. This spectrum is plotted in Fig. 13(a). The time-delay distribution of the events from which this spectrum was derived was characteristic of neutron capture.

For comparison purposes, Fig. 13(b) shows two spectra, one from a Cu^{64} source, the other of background (Table VII, columns 3, 5, and 6). The ideal background spectrum should fall monotonically from 0.2 to 0.6 Mev, being cut off sharply at the two ends of the interval. The actual pulse distribution is smeared because of noise on the traces. To make a direct comparison possible, the Cu^{64} pulses were recorded on film and measured in the same way as for the other spectra.

The spectrum of Fig. 13(a) resembles that from the β^+ source more closely than that of the background shown in Fig. 13(b). This may be taken as evidence that the first pulses were due to positron annihilation.

EVIDENCE THAT THE SECOND PULSE WAS DUE TO A NEUTRON

Evidence that the second pulses of $\bar{\nu}$-like events were due to neutrons is provided primarily by the shape of the time-delay spectrum and the effect on this spectrum of varying the cadmium concentration. Three

TABLE VII. Pulse-height spectra for first pulses.

Pulse height (Mev)	Reactor on 0.75–6 μsec	11–26 μsec	Net signal	Reactor off 0.75–6 μsec	11–26 μsec	Net rate	Net adjusted	Reactor-associated signal
0.175	96	63	74±10	4	6	1.9±2.2	8±10	66±14
0.225	281	195	213±18	16	23	8.0±4.3	36±19	177±26
0.275	521	283	422±24	34	50	16.5±6.3	73±28	349±37
0.325	582	260	491±25	38	61	16.7±6.7	74±30	417±39
0.375	516	231	435±23	33	42	18.3±6.1	81±27	354±35
0.425	395	186	330±20	43	52	23.8±7.0	106±31	224±37
0.475	281	160	225±17	33	50	15.5±6.2	69±28	156±33
0.525	236	150	183±16	23	46	7.0±5.4	31±24	152±29
0.575	120	90	89±11	16	40	2.0±4.5	9±20	80±23
0.625	49	46	33±7	9	15	3.7±3.8	16±17	17±18

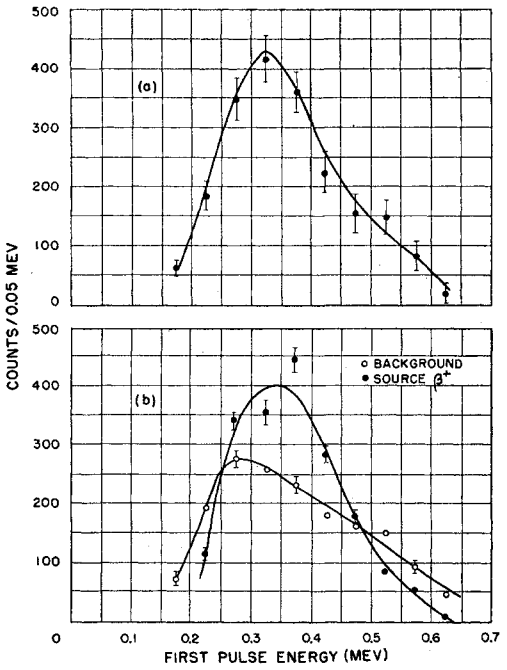

FIG. 13. (a) Pulse-height spectrum, first pulses of $\bar{\nu}$-like events. (b) Background and β^+ source spectra for comparison purposes.

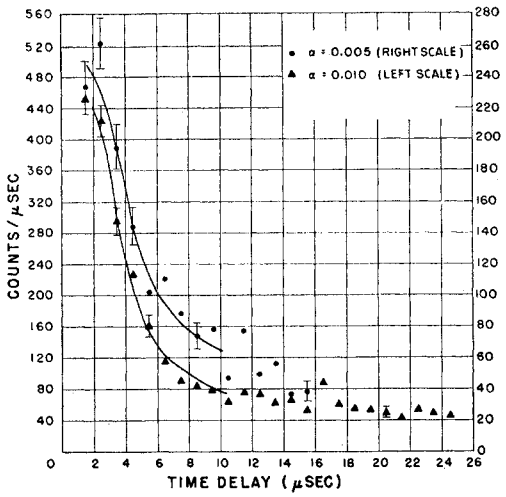

FIG. 14. Time-delay distributions of signal plus background for two different cadmium concentrations. The curves are theoretical[4] (neutron) distributions plus the calculated random background of 50 counts per channel for $\alpha=0.005$ and 0.010.

separate runs were made, with cadmium-hydrogen atomic ratios of $\alpha=0.005$, 0.010, and 0.

The time-delay spectra for $\alpha=0.005$ and $\alpha=0.010$ are shown in Fig. 14, in which the data in Figs. 7 and 8 are replotted, with the vertical scales adjusted to make comparison easier. The theoretical curves for neutron capture[4] are shown in the same figure, shifted vertically by the amount of the calculated accidental background. The time-delay distributions are in satisfactory agreement with the theoretical curves and the increase in cadmium concentration is seen to have caused a definite shift of the experimental distribution towards shorter capture times, as required.

In the case $\alpha=0$ (top triad, no cadmium in target) for 118.4 hr of running with the reactor at the same power as for the $\alpha=0.010$ case, the number of events from 0.75 to 7 μsec was 57 and the number from 7 to 27 μsec was 170.

The net number in the 0.75 to 7-μsec time interval, after subtracting the appropriate fraction (6.25/18) of the counts in the 7 to 25-μsec range, was -2 ± 8.7 or a net rate of -0.02 ± 0.07 hr^{-1}. This value is consistent with a purely random or accidental background and is to be compared with the corresponding figure for the $\alpha=0.01$ case: 1.92 ± 0.09 hr^{-1}.

Pulse-Height Spectrum

The pulse-height spectrum of the second pulses of $\bar{\nu}$-like events was examined to see if it was consistent with the spectrum to be expected from neutron capture cadmium. The method of analysis was the same as for the first-pulse spectrum, except that the pulse heights in the two detectors were added, and the same runs were used. The results are given in Table VIII.

TABLE VIII. Pulse-height spectra for second pulses.

Total energy (Mev)	Reactor on 0.75–6 μsec	Reactor on 11–26 μsec	Reactor on Net signal	Reactor off 0.75–6 μsec	Reactor off 11–26 μsec	Reactor off Net rate	Net adjusted	Reactor-associated signal
2.75	53	43	38±8	4	14	−0.9±2.4	−4±11	42±14
3.25	199	123	156±15	24	26	14.9±5.2	66±23	90±28
3.75	203	75	177±15	18	18	11.7±4.5	52±20	125±25
4.25	176	70	151±14	13	21	5.7±4.0	25±18	126±23
4.75	188	70	163±14	11	14	6.1±3.6	27±16	135±21
5.25	204	70	179±15	12	19	5.3±3.8	24±17	153±23
5.75	147	55	128±12	8	10	4.5±3.0	20±13	107±18
6.25	142	66	119±12	9	10	5.5±3.2	24±14	93±18
6.75	107	50	89±11	10	11	6.1±3.4	27±15	63±19
7.25	79	49	62±9	7	12	2.8±2.9	12±13	50±16
7.75	50	53	32±8	4	7	1.6±2.2	7±10	23±13
8.25	30	45	14±6	2	11	−1.9±1.8	−8±8	23±10
8.75	13	24	5±4	6	8	3.2±2.6	14±12	−10±13
9.25	12	34	0±4	4	8	1.2±2.2	5±10	−7±11

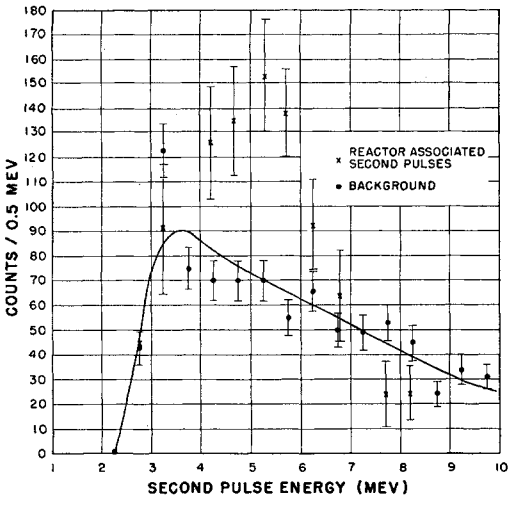

FIG. 15. Pulse-height spectrum for second pulses of $\bar{\nu}$-like events.

The pulse-height spectrum from column 9 is shown in Fig. 15, together with a background spectrum from column 3. In spite of the poor statistics, the signal spectrum can be seen to be different from the background spectrum: it appears to peak at around 5 Mev and has an end-point near 9 Mev. This supports the hypothesis that these pulses are due to neutron capture in cadmium, which releases a total energy of 9.1 Mev in gamma rays.

DEPENDENCE OF SIGNAL ON THE PRESENCE OF TARGET PROTONS

In order to see whether the signal rate was proportional to the number of target protons, an experiment was performed in which 0.47 of the target protons were replaced by deuterons. The cross section for $\bar{\nu}(d,2n)\beta^+$ relative to $\bar{\nu}(p,n)\beta^+$ for fission-spectrum antineutrinos[13] is about 1/15. Since two neutrons are produced in the first reaction, the signal rate would be expected to be decreased by a factor

$$0.53+[(2/15)\times 0.47]=0.59.$$

Target tank A was used, with the Cd/H+D) atomic ratio $\alpha'=0.010$. Since the number of electrons in the target remained essentially constant, all efficiences associated with gamma-ray transmission were unchanged. The neutron-moderation properties of the medium were different, which resulted in a change in the capture time and also altered the leakage of neutrons out of the target, and hence the capture efficiency. A calculation[4] shows that the same fraction of neutrons is expected to be captured in the interval from 0.75 to 10 μsec in the hydrogen-deuterium mixture as in 0.75 to 7 μsec in the hydrogen target.

A measurement was made of the response to a neutron source in position 5 (Fig. 9). The method was that described in the section on neutron-detection efficiency, except that an electronic time-delay analyzer was used instead of oscilloscope records. The neutron-source counts for the hydrogen-deuterium target were measured in the 0.75 to 10-μsec interval, those for the hydrogen target in 0.75 to 7-μsec. The relative detection efficiency for $(H+D)/H$ was found to be 0.9. In addition, an estimate was made of the relative neutron leakage expected for the two targets (see the section on neutron-detection efficiency). The neutron mean free path was increased to 1.24 cm for the mixed target, with the calculated result that the neutron-detection efficiency was expected to drop by the factor 0.9, in agreement with the source measurement.

The running time was 477.3 hr with the reactor on and a $\bar{\nu}$ flux factor of 1.20, and 59.9 hr with the reactor off. Figure 16 shows the observed time-delay distributions for these runs. There were 684 counts (reactor on) and 51 counts (reactor off) in the 0.75- to 10-μsec interval, giving a net reactor-associated rate of 0.58 ± 0.13 hr^{-1}.

This figure is to be compared to the rate measured with a hydrogen target and $\alpha=0.010$, given in Table II. The counting rate for the bottom triad was raised 10% to take account of its greater distance from the reactor and averaged with the rate for the top triad, giving a rate of 1.5 ± 0.02 hr^{-1} with a mean $\bar{\nu}$ flux factor of 1.14. The expected counting rate of the hydrogen-deuterium target is

$$0.59\times(1.20/1.14)\times 0.9\times(1.5\pm 0.2)=0.84\pm 0.11 \text{ hr}^{-1},$$

and the ratio of the observed to the expected rate is 0.69 ± 0.19.

Although the precision of the result leaves something to be desired, it has been shown that the reactor signal does depend on the presence of protons in the target. It is to be noted that the detection efficiency for background events is only slightly altered by the replacement of target protons by deuterons.

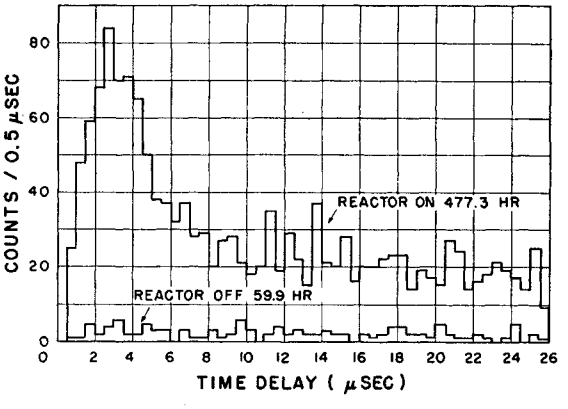

FIG. 16. Time-delay distribution for D_2O-dilution experiment. For reactor on: $\bar{\nu}$ flux factor, 1.20; counts from 0.75 to 10 μsec, 684; from 15 to 25 μsec, 387. For reactor off: counts from 0 to 10 μsec, 51; 15 to 25 μsec, 38.

[13] C. L. Cowan, Jr., and F. Reines, Phys. Rev. **107**, 1609 (1957).

This experiment also indicates that there is no marked contribution to the reactor-associated signal from $\bar{\nu}$ events which took place in the hydrogenous scintillator liquid of the detectors or in the plastic target. Contributions from events in the detectors are not expected to be important because of the decreased probability both of positron and neutron detection in such events. Contributions from events in the plastic target tank would be expected to amount to less than 13% or $\frac{1}{2}$ the ratio of plastic thickness to target thickness.

ARGUMENTS AGAINST NEUTRONS AS THE CAUSE OF THE REACTOR-ASSOCIATED SIGNAL

It was possible for fast neutrons from the reactor to cause a delayed coincidence having many of the characteristics which we ascribe to an antineutrino event. This can be imagined to happen as follows: A fast neutron makes a collision with a proton in one of the detector tanks and causes a pulse, the neutron then passes through the water target, collides in the other detector of the triad and makes a pulse in time coincidence with the first (i.e., within 0.2 μsec, the resolving time of the system), and then diffuses back to the water target, where it is captured by the dissolved cadmium. The sequence pictured is not very probable and experiments with fast-neutron sources (Pu–Be, Am–Be) external to the H_2O target show that the primary effect of such a source is to increase the accidental background. Less than one-half of the delayed coincidences due to the source have the time distribution characteristic of neutrons.

Since the reactor-associated rise in the accidental background is not more than 1/25 of the reactor-correlated signal, we conclude that not more than this fraction of the signal is due to neutrons from the reactor. This argument has to take account of the difference in the spectrum from the reactor as compared to that from the neutron sources since higher energy neutrons would be more effective in producing the kind of delayed coincidence described above. However, the mean energy characteristic of the fission process is 2 Mev,[14] as compared with that from the neutron source of about 4.5 Mev,[6] and the effect of the massive shield between the reactor and the detector is to decrease the mean energy of the neutrons which penetrate it.

This argument is presented in addition to the more direct total-absorption measurement described in the next section. The heavy-water-dilution experiment also bears on this question because in it the reactor-associated signal dropped greatly although the neutron-detection efficiency was essentially unchanged, ruling out reactor neutrons. Finally, the lead-absorption experiment proves that the signal could not have been produced by neutrons since they would not have been appreciably degraded in passing through a 0.95-cm lead sheet. The predicted decrease in signal would have been given by column 3 rather than column 4 of Table VI, in disagreement with the observations.

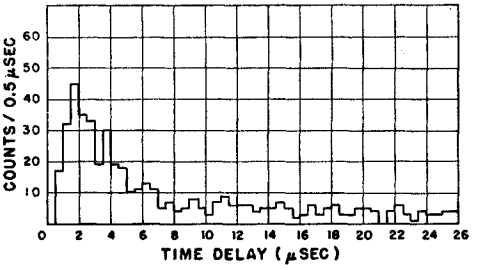

FIG. 17. Time-delay distribution for sawdust-shielding experiment. For reactor on: $\bar{\nu}$ flux factor, 1.21, counts from 0.75 to 7 μsec, 293; from 11 to 26 μsec, 123. Total run time, 127.7 hr.

TOTAL-ABSORPTION TEST OF REACTOR-ASSOCIATED SIGNAL

The only known particles other than antineutrinos which are capable of being produced by the fission process and a secondary reaction external to the detector are gamma rays, electrons, protons, and neutrons. A direct test of the reactor-associated signal is to measure how it is affected by neutron and gamma-ray shield. Protons and electrons are automatically excluded as the source of the signal if these more penetrating radiations can be ruled out. If the signal is due to antineutrinos, it will, of course, not be affected by the shield. An experiment was done in which the correlated delayed coincidence rate was measured with and without a shield of 76 cm of wet sawdust in bags (density 0.52 g/cm^3).[15] The signal with the shield was measured with the top triad to be 1.86 ± 0.13 hr^{-1}, or 1.74 ± 0.12 hr^{-1} after adjusting it for the difference in $\bar{\nu}$ fluxes for identical runs without the shield. This number is to be compared with 1.69 ± 0.17 hr^{-1} for the runs with no shield. Figure 17 shows the time-delay distribution curve for this experiment.

The detector was surrounded by a lead shield (Fig. 2) and located between two massive concrete walls several feet thick. The roof of the detector chamber was also a heavy shield of concrete and water; the floor was based on the ground. This left two openings which were much less well shielded from the reactor, i.e., the front and back of the detector. Our sawdust shield was placed in front and back, overlapping by a few feet the edges of the heavy shielding already there. The sawdust shield was 2.5 mean free paths (mfp) thick in the shortest dimension for 10-Mev neutrons and some 50 mfp

[14] Cranberg, Frye, Nereson, and Rosen, Phys. Rev. **103**, 662 (1956).

[15] With shield total run time, 127.7 hr; $\bar{\nu}$ flux factor, 1.21. Without shield (top triad only): total run time, 417.9 hr; $\bar{\nu}$ flux factor, 1.13. See Table II.

thick for thermal neutrons. For gamma rays it was more than 1.5 mfp for energies below 10 Mev and more than 3 mfp for energies below 2 Mev. It should therefore have reduced fast neutrons from the reactor by at least a factor of 10 and gamma rays by a factor of 5 or more.

The effectiveness of the shield was checked by means of an Am—Be neutron source placed in a standard position outside the lead shield door. The singles rate of the detector response to the neutron source was measured in the energy range from 0.1 to 0.5 Mev with and without the sawdust shield. Counts in this range are due to neutron recoils and capture gamma rays. The shield reduced the count rate in this energy range by two orders of magnitude. The lack of appreciable change in the counting rate after installation of the sawdust shield is evidence that the signal was not due to neutrons or gamma rays produced outside the detector.

CONCLUSIONS

We have in these experiments demonstrated in a somewhat redundant manner the presence of a reactor-associated signal of the expected magnitude and with the detailed characteristics of the reaction $p(\bar{\nu},\beta^+)n$. Tests were made of the signal to show that the first pulse of the characteristic delayed-coincidence event was due to positron annihilation and the second pulse to neutron capture in the cadmium of the water target. It was also demonstrated that the signal depended on the presence of the target protons in the sense that the signal could be diminished by eliminating some of the $\bar{\nu}$ targets. A final test of the signal was made by means of a classical total-absorption experiment in which reactor-associated particles other than antineutrinos were ruled out.

ACKNOWLEDGMENTS

We are indebted to a great many people for their contributions to this experiment: Dr. A. R. Ronzio for his work on scintillator development; R. P. Jones and M. P. Warren for mechanical maintenance and assembly of the equipment at Los Alamos and Savannah River; C. W. Johnstone and members of LASL Group *P*-1 for design and construction of the electronics; A. T. Brousseau for putting the electronics into final operating condition; W. H. Borkenhagen for mechanical design of the tanks and auxiliary equipment, and the LASL Shops Department for actual construction of the detectors, shields, and storage tanks; the Purchasing and Shipping Department of LASL for invaluable logistic support in obtaining and moving many tons of equipment across the country from Los Alamos to Savannah River. We wish also to thank the E. I. du Pont de Nemours Company, which operates the Savannah River Plant of the U. S. Atomic Energy Commission, for their hospitality.

APPENDIX I. DETAILS OF BACKGROUNDS

Double Compton Scattering

It is interesting to note that the accidental backgrounds in the prompt coincidence gates, N_β and N_n, were in large part due to double Compton scattering of gamma rays, once in each detector. For example, in one run (with filled target tank *A* in position) the single counting rates in the β gates were: 1β, 1030 sec^{-1}; 2β, 530 sec^{-1}. The calculated rate of accidental coincidences is $2(1\beta)(2\beta)\tau=2.2$ sec^{-1}, where $\tau=0.2$ μsec is the resolving time. The N_β rate was 5.9 sec^{-1}. The N_β and N_n rates rose by a factor 2.0 and 1.5, respectively, when the target tank was removed, indicating an increased correlation between the two detectors in this case.

Long Upper Gate

The characteristics of our amplifiers were such that an overloaded pulse had a "bustle" about 10% of the maximum pulse height, and with a length dependent on the degree of overload; the bustle length was about 10 μsec for each factor of 10 overload. At the end of this bustle were small pulses capable of tripping the discriminators. A "long upper gate," which paralyzed the circuit for a specified time following a large pulse, was designed to eliminated false coincidences due to small pulses riding on the tails of large pulses (due to cosmic rays or electrical noise). The long upper gate was at first 28 μsec long. It was lengthened to 100 μsec for part of the first series. During the second series it was fixed to stay on until 60 μsec after the pulse had returned to the baseline. This reduced both the dead time of the system due to the long upper gate, and the number of unacceptable films due to pulses riding on bustles.

Cosmic-Ray Background

Cosmic-ray particles that passed through the detectors in a way that made a coincidence in most cases gave pulses close to 100 Mev [Fig. 6(b)]. Relativistic particles passing through the "nonscintillating" liquid between the photomultiplier faces and the plastic window, or through the photomultipliers, made pulses by the Čerenkov effect and the residual scintillation properties of these media. These pulses might fall in the "neutron" or "positron" energy gates and thus cause a false coincidence. To reduce the number of such events, before run 28 the pure triethylbenzene medium behind the plastic windows of tank 2 was replaced with one-half strength scintillating solution. It was hoped that pulses which fell in the n or β^+ energy gates in tank 1 or 3 would now be much too big in 2, and hence be rejected. These cosmic ray events could sometimes be recognized by the appearance of coincident pulses in all three detector tanks. Pictures of this sort [Fig. 5(e), 5(f)] were rejected. Of course, those

which missed the third tank could not be recognized in this way. Since the N_n and N_β rates included these cosmic-ray events, there was a small overcorrection for accidental background, both with the reactor on and off. Since the N_β and N_n rates were slightly higher with the reactor on than off, the overcorrection was not exactly compensated in the on-off subtraction.

APPENDIX II. NEUTRON ENERGIES EXPECTED FROM $\bar{\nu}$ REACTION

The detailed neutron spectrum can be derived from the two-component neutrino theory and the $\bar{\nu}$ spectrum. However, for our purposes we only require limits on the expected spectrum to be able to establish a semi-quantitative guide for the interpretation of our results. It is clear from momentum-balance considerations that the large mass of the product neutron relative to that of the product β^+ will result in only a small fraction of the available energy going to the neutron.

From the energy-momentum conservation laws, the maximum energy, E_n, a product neutron can attain for a given $\bar{\nu}$ energy, E_ν, is given by the approximate expression

$$E_n=(m/2M)\{E_\nu+[(E_\nu-Q)^2-1]^{\frac{1}{2}}\}^2, \qquad (4)$$

where m/M is the ratio of electron to neutron mass and $Q(=2.52)$ is the threshold energy for the reaction excluding the β^+ rest energy. All energies are in units of the electron rest energy and we have neglected E_n/E_ν.

The neutron produced by an average $\bar{\nu}$, i.e., with an energy about 3 Mev, has an upper limit for energy of 12 kev. Further consideration of the conservation equation shows that the minimum energy a product neutron can acquire is 1.9 kev; even at threshold the conservation of momentum requires the neutron to carry off some momentum and hence energy.

APPENDIX III. EXPECTED β^+ SPECTRUM AND β^+ LEAKAGE FROM TARGET

In order to estimate the effect on β^+-detection efficiency of β^+ leakage from the target, we must first know the energy spectrum, $n(E_\beta)$. This is deduced from the $\bar{\nu}$ spectrum, $N(E_\nu)$, inferred from the fission-fragment β^- spectrum,[12] $n(E_\beta)$, and the cross section, $\sigma(E_\nu)$, for reaction (1):

$$\sigma(E_\nu)=A(E_\nu-Q)[(E_\nu-Q)^2-1]^{\frac{1}{2}}, \qquad (5)$$

$$N(E_\nu)=B[n(E_\beta)/\sigma(E_\beta)], \qquad (6)$$

where

$$E_\beta=E_\nu-3.52.$$

The unit of energy is the electron rest energy, E_β is the β^+ kinetic energy, E_ν is the $\bar{\nu}$ energy, and A and B are normalization factors with values that do not concern us here. The neutron kinetic energy has been neglected. Figure 18 shows the predicted positron spectrum. An upper limit for the effect of positron leakage for the target can be obtained by assuming that all positrons that leave the target are not detected. Computing the leakage for the average β^+ (2 Mev, range of 1.5 cm) with an isotropic angular dependence generated uniformly throughout an infinite slab 7.6 cm thick, we find it to be 0.09. This figure represents a gross overcorrection to the β^+-detection efficiency because those β^+ which leave the target can still be detected, though with a slightly smaller efficiency. Further, neutrons generated near the target surface are more likely to leak out than those originating near the center, so that β^+ generated near the slab surface are not favored in contributing to a $\bar{\nu}$ event. Leakage from an infinite slab probably lowers the β^+-detection efficiency by less than a few percent. Edge leakage from the actual target tanks has a negligible ($<1\%$) effect on the efficiency.

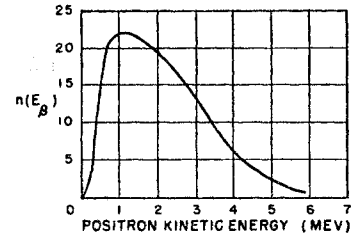

FIG. 18. Predicted kinetic-energy spectrum of positrons generated in the reaction $p(\bar{\nu},\beta^+)n$.

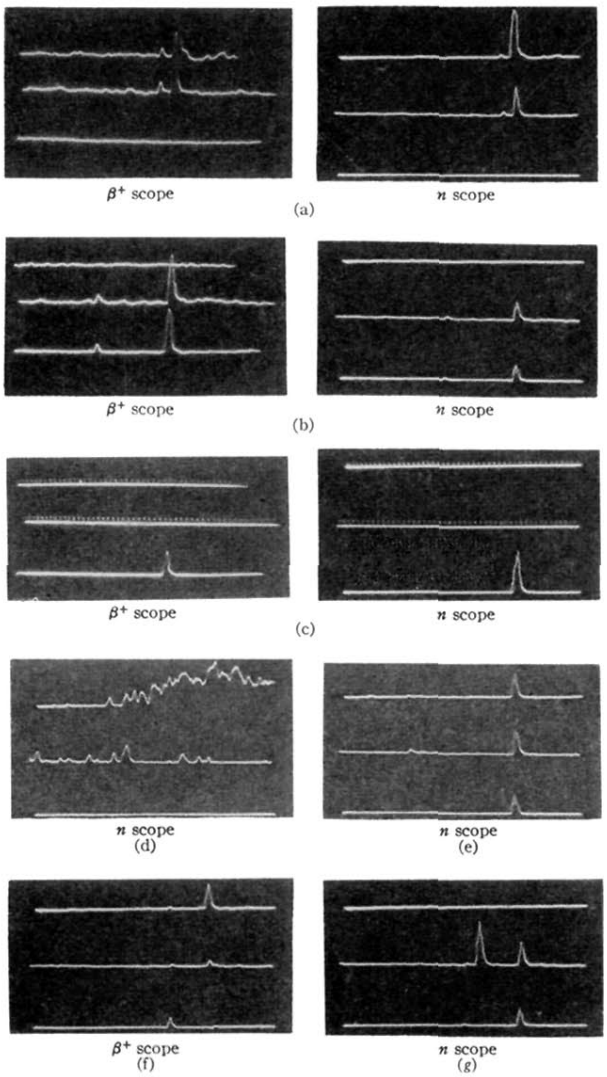

FIG. 5. Sample scope pictures. (a) and (b) are acceptable frames (possible $\bar{\nu}$ events); (c) shows a set of calibration traces; and (d) through (g) are not acceptable. (a) Event in top triad. Delay, 2.5 μsec. First pulse, 0.30 Mev in 1, 0.35 Mev in 2. Second pulse, 5.8 Mev in 1, 3.3 Mev in 2. (b) Event in bottom triad. Delay, 13.5 μsec. First pulse, 0.25 Mev in 2, 0.30 Mev in 3. Second pulse, 2.0 Mev in 2, 1.7 Mev in 3. (c) 0.5-μsec timing markers on traces 1 and 2, 5-Mev (n scope) and 1-Mev (β scope) calibration markers on trace 3. (d) Electrical noise. (e) Cosmic-ray event, "neutron triple." (f) Cosmic-ray event "positron triple." (g) Event, possible due to cosmic rays. Rejected because of an extra pulse but otherwise acceptable. Frames like this occurred more often than would be expected from chance coincidences, but not often enough so that their omission would affect the results appreciably.